CHAPTER IV
RESULTS AND DISCUSSION

4.1 Critical Micelle Concentration and Average Micelle Radius

Cheong and Panagiotopoulos (Cheong et al. 2006) studied the micellization of SDS with a series of simulations . We also used a set of simulations to determine the critical micelle concentration (CMC) of the coarse-grained surfactant. We simulated a series of surfactant-water systems at increasing surfactant concentration.. At 0.00468 surfactant molecules per nm^3 (correspondent to 7.77 mmols/liter) we observed the formation of the first micelle. At this concentration all surfactants present within our simulation box were found within the micelle, and no free surfactant was observed. As the surfactant concentration was increased further, more micelles formed, as detailed in Table 4.1

Table 4.1 Number of micelles in SDS-water systems.

Simulation #	Concentration (mmols/liter)	Number of micelle present
1	7.77	1
2	8.84	2
3	9.92	2
4	11.11	3
5	12.19	3
6	13.27	3
7	15.54	4
8	17.7	3
9	19.9	4
10	22.11	4
11	44.22	9
12	66.45	9
13	88.56	15

Table 4.1 Number of micelles in SDS-water systems. (cont.)

Simulation #	Concentration (mmols/liter)	Number of micelle present
14	110.67	18
15	221.35	30
16	332.02	35
17	442.7	47

We analyzed our simulation results to determine the average size of the micelles in the surfactant-water simulations. The results are shown in Fig. 4.1; the average micelle radius was ~2.018 nm.

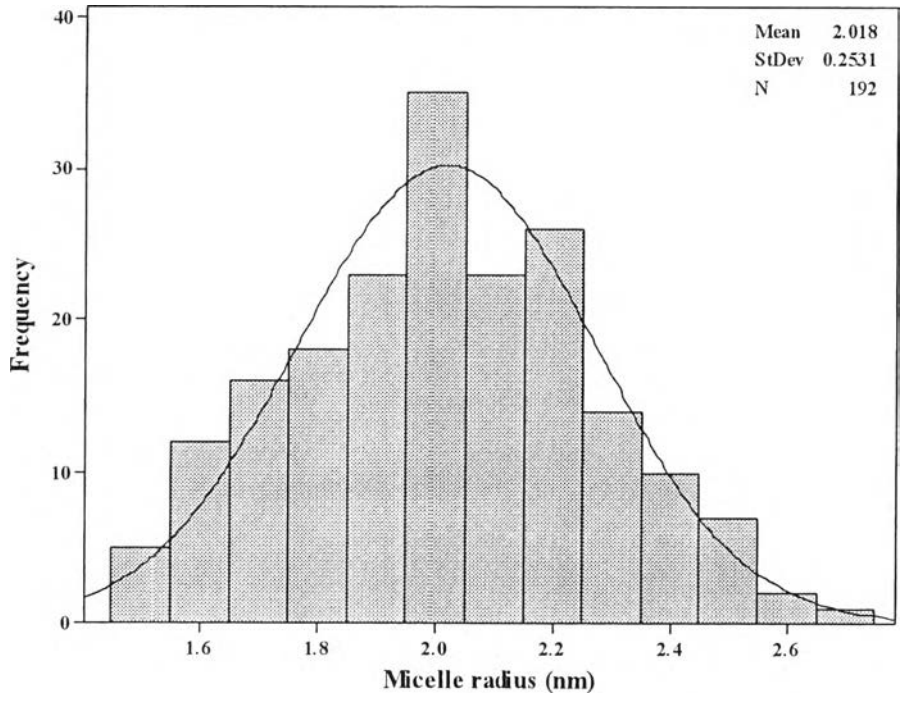

Figure 4.1 Micelle radius distribution in this simulation.

The average micelle radius is in good agreement with the experimental result from neutron scattering obtained by Cabane and coworkers (Cabane et al. 1985). The experiment was conducted with the SDS-water solution at the concentration of 69.35 mmol/liter, at room temperature, and the micelle radius was 1.84 nm. This value is also comparable with results

obtained from coarse-grained simulation by Jalili and Akhavan (micelle radius = 2.03 nm) (Jalili et al. 2009) and molecular dynamics simulations by Bruce and coworker (micelle radius = 2.09 nm) (Bruce, Berkowitz et al. 2002) and by Mackerell (micelle radius = 1.97 nm) (Mackerell 1995)

4.2 Orientation

Regarding surfactants adsorbed on GS and GN, we calculated the average polar angle, represented schematically in Fig. 4.2. The angles were calculated from the trajectories of the last 0.1275 ns of the 1.1475 μs-long simulations. During this time, there was no SDS molecule leaving from the surface.

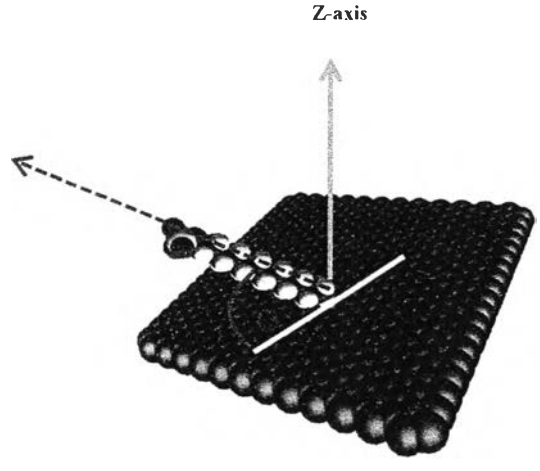

Figure 4.2 The three dimensional orientation angle Θ between SDS and surface.

The angle Θ ranges from 0° to 90°. When the angle Θ is equal to 0°, the SDS molecule is parallel to the surface, and when the angle Θ is 90°, the surfactant is perpendicular to the surface. The angle distributions of SDS molecules on different surfaces, at the surface coverage of 0.5 nm^2/SDS molecule, are shown in Fig. 4.3

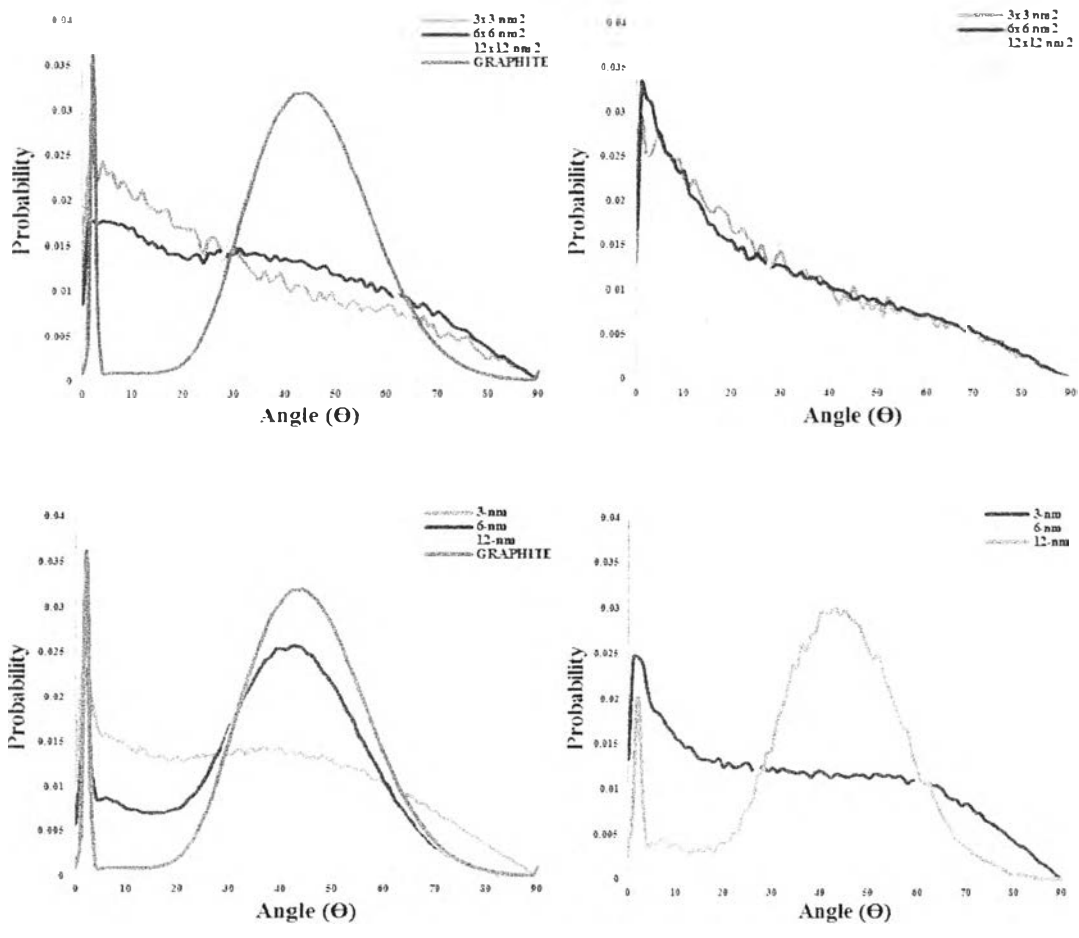

Figure 4.3 Angle distribution of SDS molecules on GS (Top-left), GOS (Top-right), GN (Bottom-left) and GON (Bottom-right). The angle distribution of SDS molecules on graphite is plotted to compare with the angle distribution on GS and GN.

The snapshots of the SDS aggregate on different GSs, at equilibrium, are shown in Fig. 4.4. The snapshots of DPD simulations have less presentation quality, compared with the snapshots of MD simulations, because the details of the molecules have been simplified into spheres.

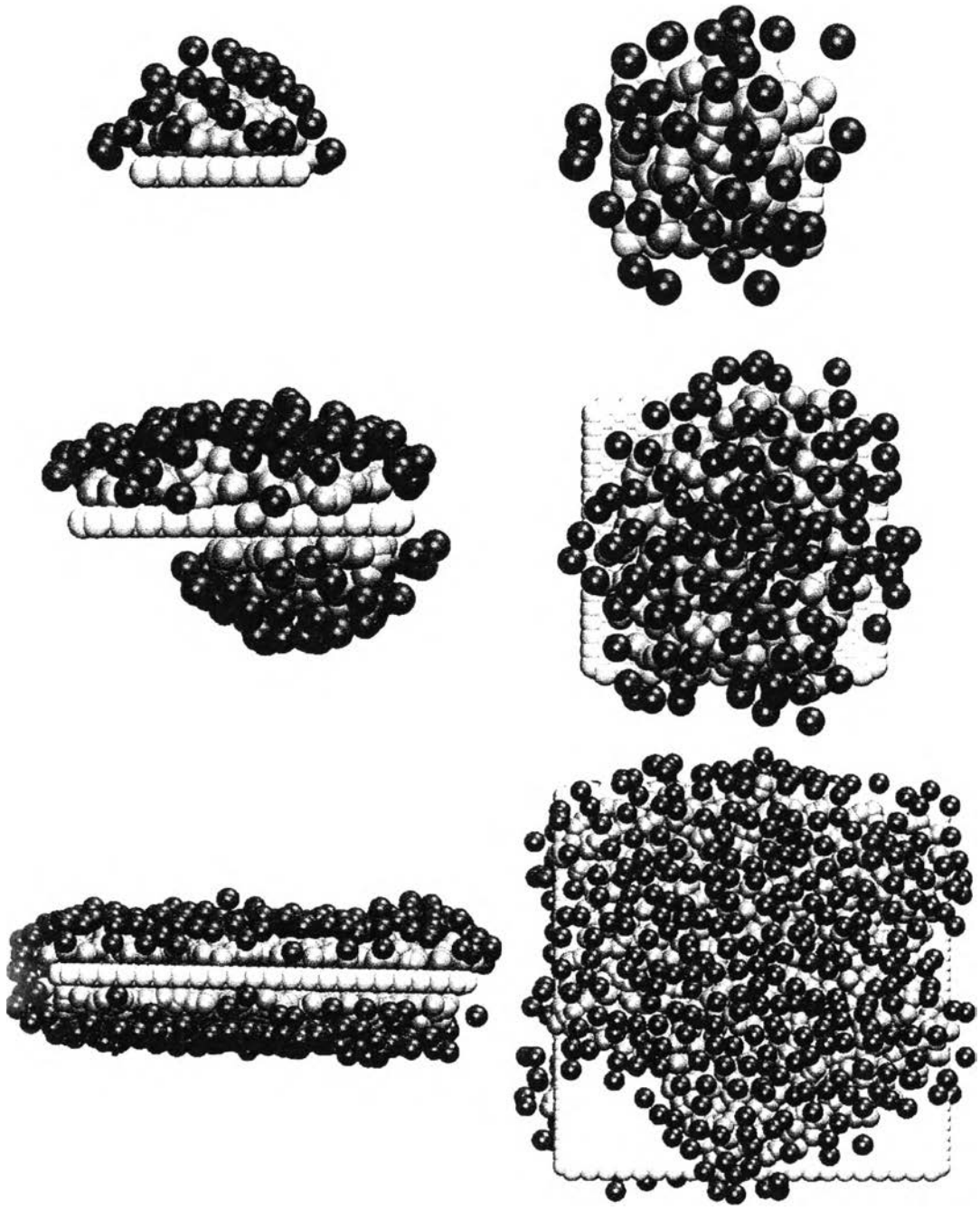

Figure 4.4 Side (left panel) and top (rigth panel) views of SDS aggregate on GS of different sizes, at equilibrium. The first row represents 3×3 nm^2 GS. The second row represents 6×6 nm^2 GS, and the third row represents 12×12 nm^2 GS. Hydrophobic tail beads are in green color, hydrophilic head beads are in purple color, and graphene beads are in light grey color. The coverage of all the sheets is 0.5 nm^2/SDS molecule.

The visual inspection of the snapshot of the SDS aggregate on GSs indicates that when the size of the GS is small, the aggregate can move from one side and merge with the another aggregate on another side of the sheet after a certain period of

simulation time (Wu et al. 2012). On the 3×3 nm^2 GS, the surfactants are forced to stack on each other to minimize the contact between the hydrophobic-tails and water. This results in multi-layered hemispherical aggregate formation. The angle distribution of the aggregate on the 3×3 nm^2 GS is consistent with the aggregate's snapshot, since the distribution implies the hemispherical (or spherical) shape.

On the 6×6 nm^2 GS, the aggregate still possesses the curvature, with wider angle, and multi-layered structure (Tummala, Grady et al. 2010). The decrease of the aggregate curvature corresponds to the change of orientation of the SDS molecules. The surfactants preferably orient themselves to the angles in range of 20° to 70°; changing the orientation trend.

On the 12×12 nm^2 GS, the aggregate becomes more like a monolayer structure. The surfactants adhere directly with the surface rather than stacking on each other. They orient themselves in the range of 20° to 70°, around the center of the sheet; resulting in the apparently flat aggregate in the middle of the sheet. Nevertheless, the surfactants still lie parallel around the edge of the aggregate.

The SDS angle distribution plots suggest that the width of the GN has an effect on the orientation trend of SDS aggregate. The snapshots of the aggregate on GNs are shown in Fig. 4.5. These snapshots are different from the snapshots in Fig. 7 because the side views of the GNs are infinitely long, so these sheets have same lengths in snapshots. However, their widths are different, as we observe from the top view.

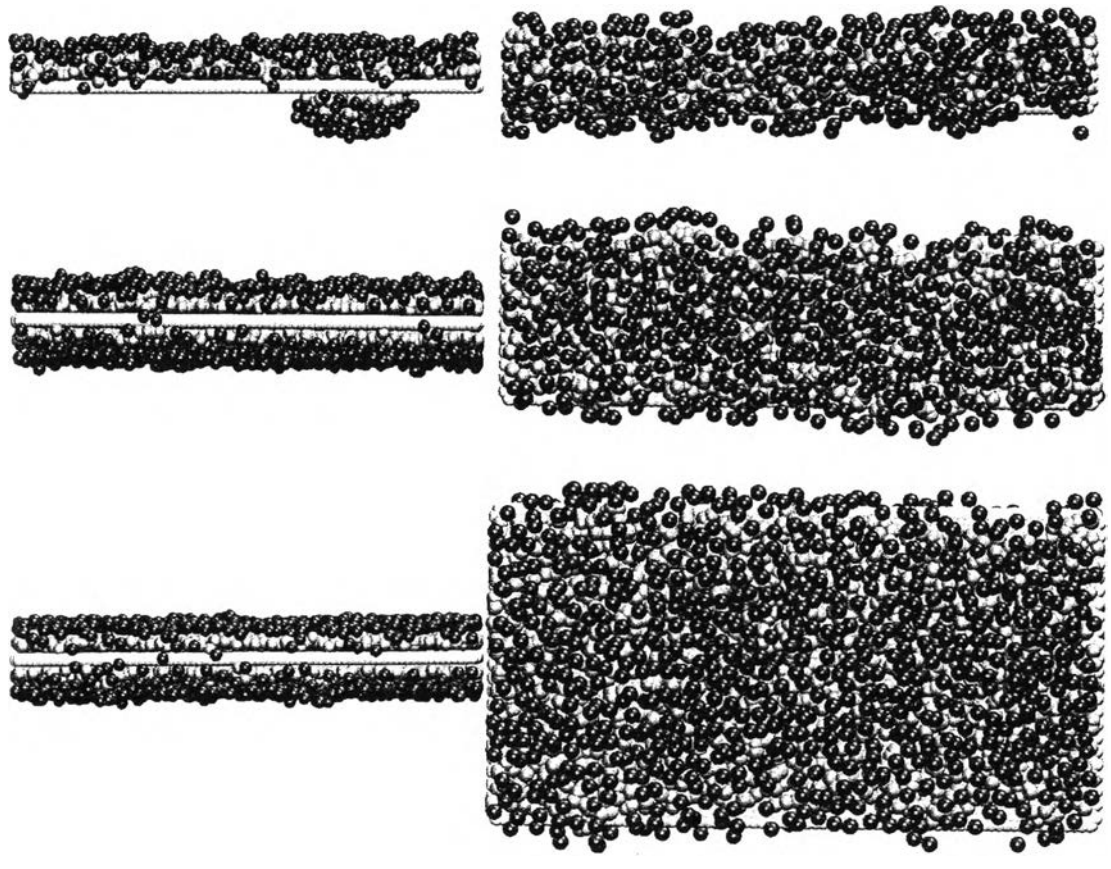

Figure 4.5 Side (left panel) and top (rigth panel) views of SDS aggregate on GN of different widths, at equilibrium. The first row represents 3-nm wide GN. The second row represents 6-nm wide GN, and the third row represents 12-nm wide GN. Hydrophobic tail beads are in green color, hydrophilic head beads are in purple color, and graphene beads are in light grey color. The coverage of all the sheets is 0.5 nm^2/SDS molecule.

On 3-nm wide GN, the unequal amount of aggregate on each side can be observed. This happens due to small width of the nano-ribbons that allows the aggregate to move from one side to another side easily. The punctual formation of multi-layered structure can be seen along the aggregate, due to limited width of the nano-ribbon. However, the main feature of the aggregate is the perpendicular alignment of flat SDS molecules along the edges of the nano-ribbon. (Tummala,

Grady et al. 2010). This phenomenon contributes to dominant population of parallel-angled surfactants, as shown in the angle distribution plots.

Similar to the case of GS, when the width of the surface increases, the aggregate tends to lose its curvature, as the surfactants in the middle of the surface directly adsorb on the nano-ribbon's surface (Tummala, Grady et al. 2010), and orient in the angles of the range 20° to 70°; forming monolayer structure, as seen in Fig. 9. The angle distribution of the flat SDS molecules remains virtually constant, whereas the angles between the 20° and 70° increases, and the other angles apart from these angles decreases. The trend of the SDS orientation on GN resembles the orientation on graphite, unlike GSs This indicates that the presence of edges can manipulate the orientation trend of the surfactants on the surface.

With the presence of pseudo-oxide edges, the orientations and morphology of SDS aggregate on both GOS and GON are affected. The snapshots of the SDS aggregate on GOSs are shown in Fig. 4.6

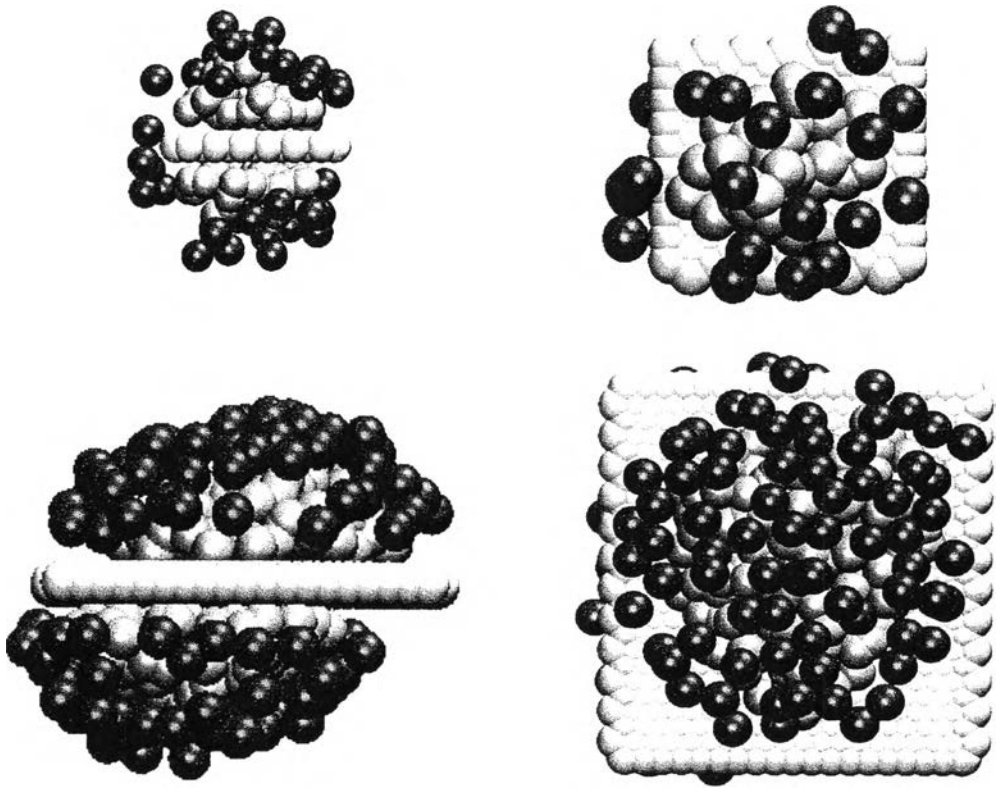

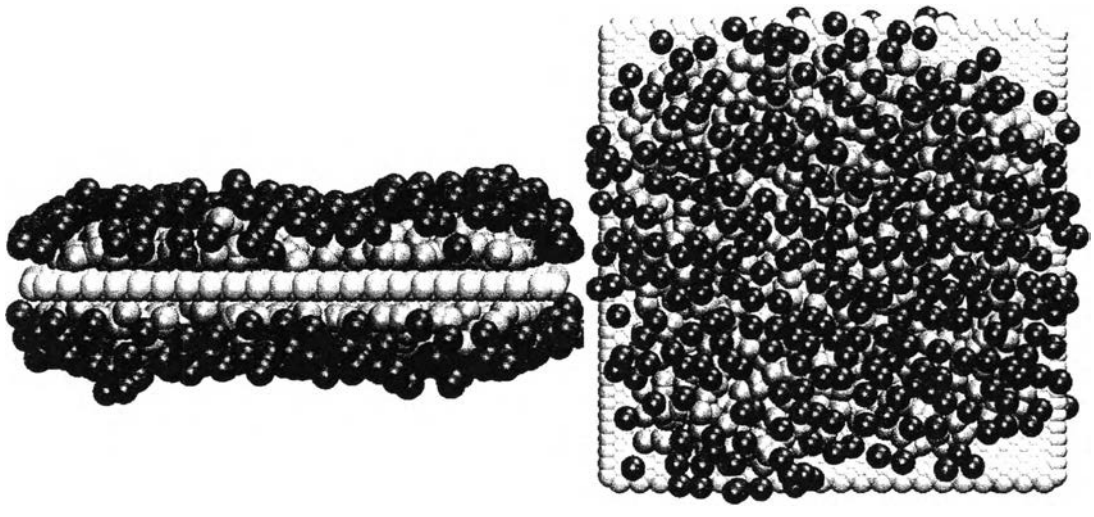

Figure 4.6 Side (Left panel) and top (rigth panel) views of SDS aggregate on GOS of different sizes, at equilibrium. The first row represents 3×3 nm^2 GOS. The second row represents 6×6 nm^2 GOS, and the third row represents 12×12 nm^2 GOS. Hydrophobic tail beads are in green color, hydrophilic head beads are in purple color, graphene beads are in light grey color, and pseudo-oxide edges are in brown color. The coverage of all the sheets is 0.5 nm^2/SDS molecule.

The first apparent effect of the pseudo-oxide edge is preventing the movement of the aggregate from one side to another side. The aggregates are restricted to be on their respective sides due to simultaneous high attraction between the hydrophilic head beads and pseudo-oxide edges, and high repulsion between the hydrophobic tail beads and pseudo-oxide edges, thus the aggregates are present equally on both sides of the GOSs. The restriction of the aggregate migration can be useful in controlling the dispersion of GOS in aqueous solution (Dong et al. 2011), since the presence of the aggregate can reduce the attraction between the GOSs.

The morphology of the aggregate on 3×3 nm^2 GOS is different from the aggregate on 3×3 nm^2 GS, due to different amount of surfactants present in the aggregates of each case. In the case of 3×3 nm^2 GOS, the aggregates contain fewer SDS molecules, but still exhibit the multi-layered structure. This is related to the restriction effect of the pseudo-oxide edges that forces the hydrophobic tails to stay

away from the edge, inside the boundary, and forces the hydrophilic heads to be close to the edges. Therefore the base layer of the multilayered aggregate is forcefully created, with fewer surfactants. The restriction of the hydrophobic tails can be seen on every GOS, as none of them touches the edges.

Due to the presence of aggregate on both sides of the GOS, the angle distribution of parallel SDS molecules, which act as a base layer of the aggregate, increases. The similar phenomenon occurs on 6×6 nm^2 GOS, when the presence of multilayered aggregate on both sides of the sheet increases the population of parallel SDS molecules. However, the orientation of SDS on 12×12 nm^2 GOS is not so different from the orientation of SDS on 12×12 nm^2 GS, because the size of the sheet is too big for the edges to have an apparent effect on the aggregates. When the size of GOS increases, the hydrophilicity of the pseudo-oxide edges becomes negligible compared with the hydrophobicity of the rest of the sheet (Hu et al. 2013).

The snapshots of the aggregate on GONs are shown in Fig. 4.7. In the case of GONs, equal amount of aggregate can be observed on both sides, because the aggregates are restricted by the pseudo-oxide edges. The hydrophobic tail beads are visibly away from the edges, as they are on the GOSs' surface, therefore the aggregates are affected in the similar way as they are affected on GOSs. However, due to the presence of fewer edges, the effect that the pseudo-oxide edges have on the orientation of SDS on 6-nm wide and 12-nm wide GONs is almost insignificant

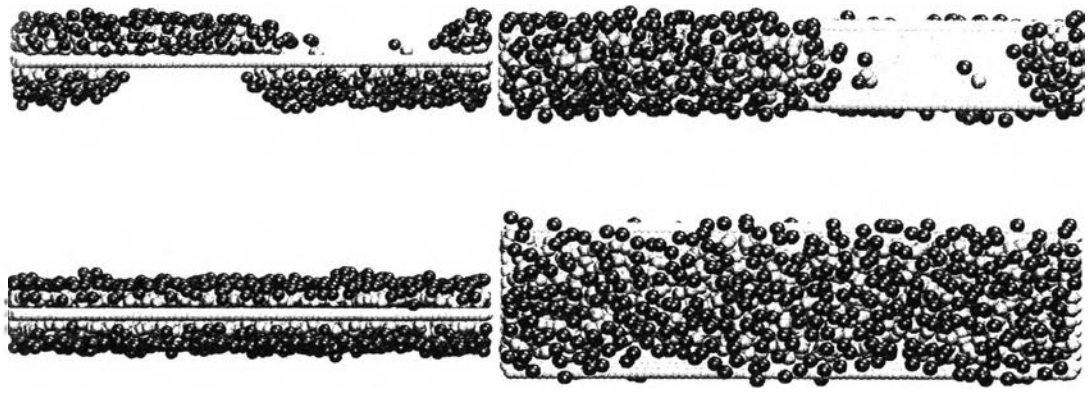

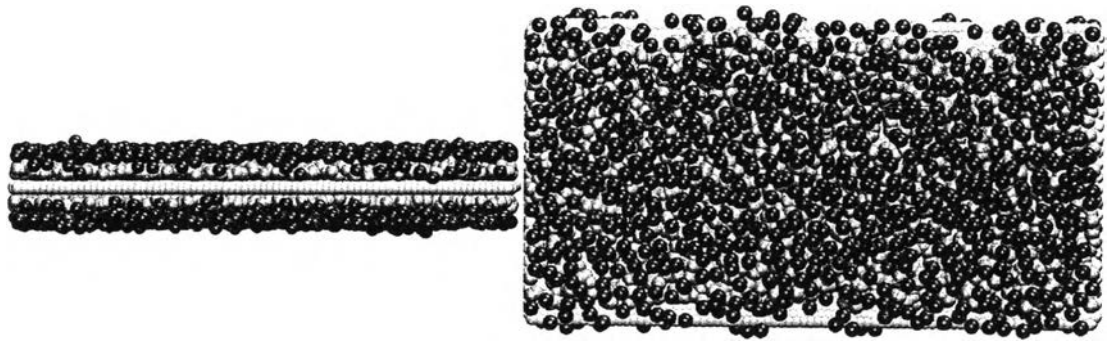

Figure 4.7 Side (left panel) and top (rigth panel) views of SDS aggregate on GON of different widths, at equilibrium. The first row represents 3-nm wide GON. The second row represents 6-nm wide GON, and the third row represents 12-nm wide GON. Hydrophobic tail beads are in green color, hydrophilic head beads are in purple color, graphene beads are in grey color, and pseudo-oxide edges are in brown color. The coverage of all the sheets is 0.5 nm^2/SDS molecule.

4.3 Order parameter

An order parameter (S) was calculated using the second Legendre polynomial (Wilson 1996) of the cosine of angle θ between the average orientation vector of every SDS molecules within the aggregate and individual orientation vector of each SDS molecule in the aggregate ($S = \langle \frac{3cos^2\theta - 1}{2} \rangle$). If the value of the order parameter is close to 1, the surfactants in the aggregate orient within same angle respect to the surfaces. Vice-versa when S approaches 0. The aggregate can have high order parameter value if there is narrow specific range of orientation angles. The presence of various orientation angles reduces the order parameter of the aggregate. The average order parameters obtained during the last 0.1275 ns of the 1.1475 μs-long simulations are shown in Fig. 4.8

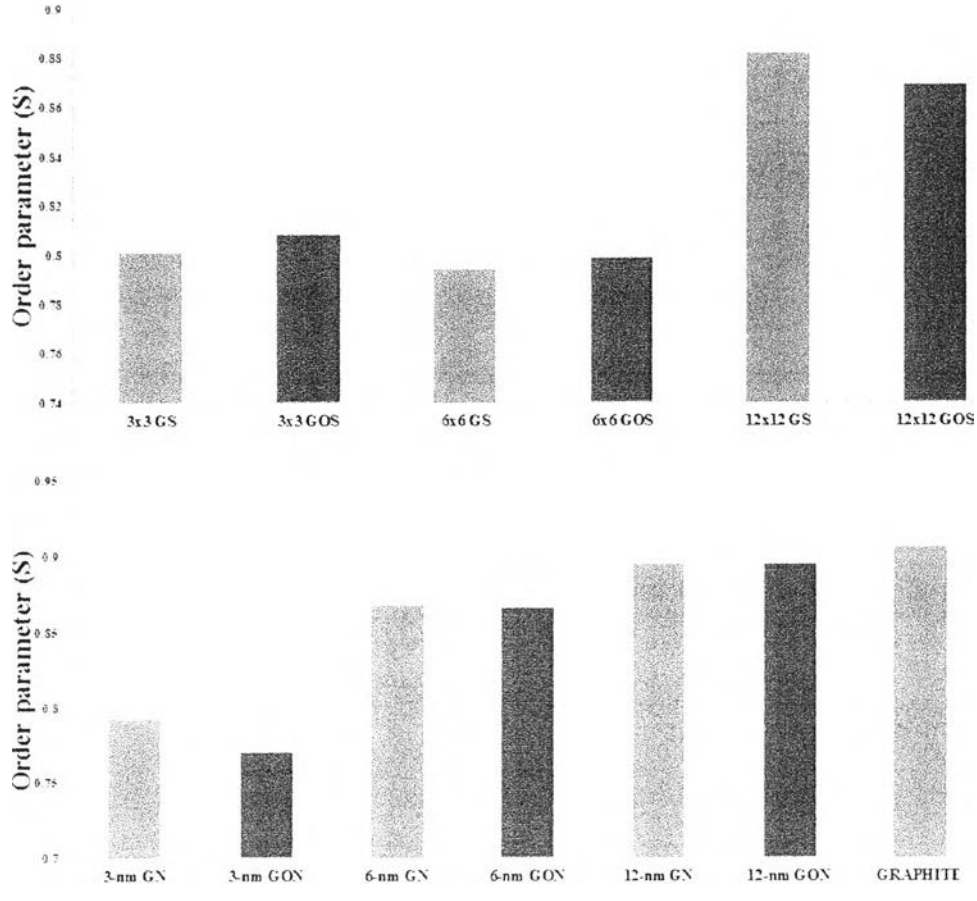

Figure 4.8 Order parameter of surface aggregate on different sheets (Top panel) and different nano-ribbons (Bottom panel). Blue columns represent the nano-particles without pseudo-oxide edges, and red columns represent the nano-particles with pseudo-oxide edges.

The order parameter reduces as the size of the surface decreases, because of the effect of lateral confinement that forces the micelle to be spherical, and simultaneously, force the surfactants to point in different directions and become more isotropic (Tummala, Grady et al. 2010). However, this result is imperfect, because the angles used to calculate this parameter do not indicate the directions. The SDS molecules that make the same angle along Z-axis may point in the different direction along X-axis and Y-axis.

4.4 Density profiles

One-dimensional density profiles of head and tail groups, as the function of the perpendicular distance from the carbonaceous surfaces, are shown in Fig. 4.9. Only the surfactants in the surface aggregate, which were within the limits of 3 nm orthogonal to the surfaces, were calculated. The profiles were calculated from the trajectories of the last 0.1275 ns of the 1.1475 μs-long simulations

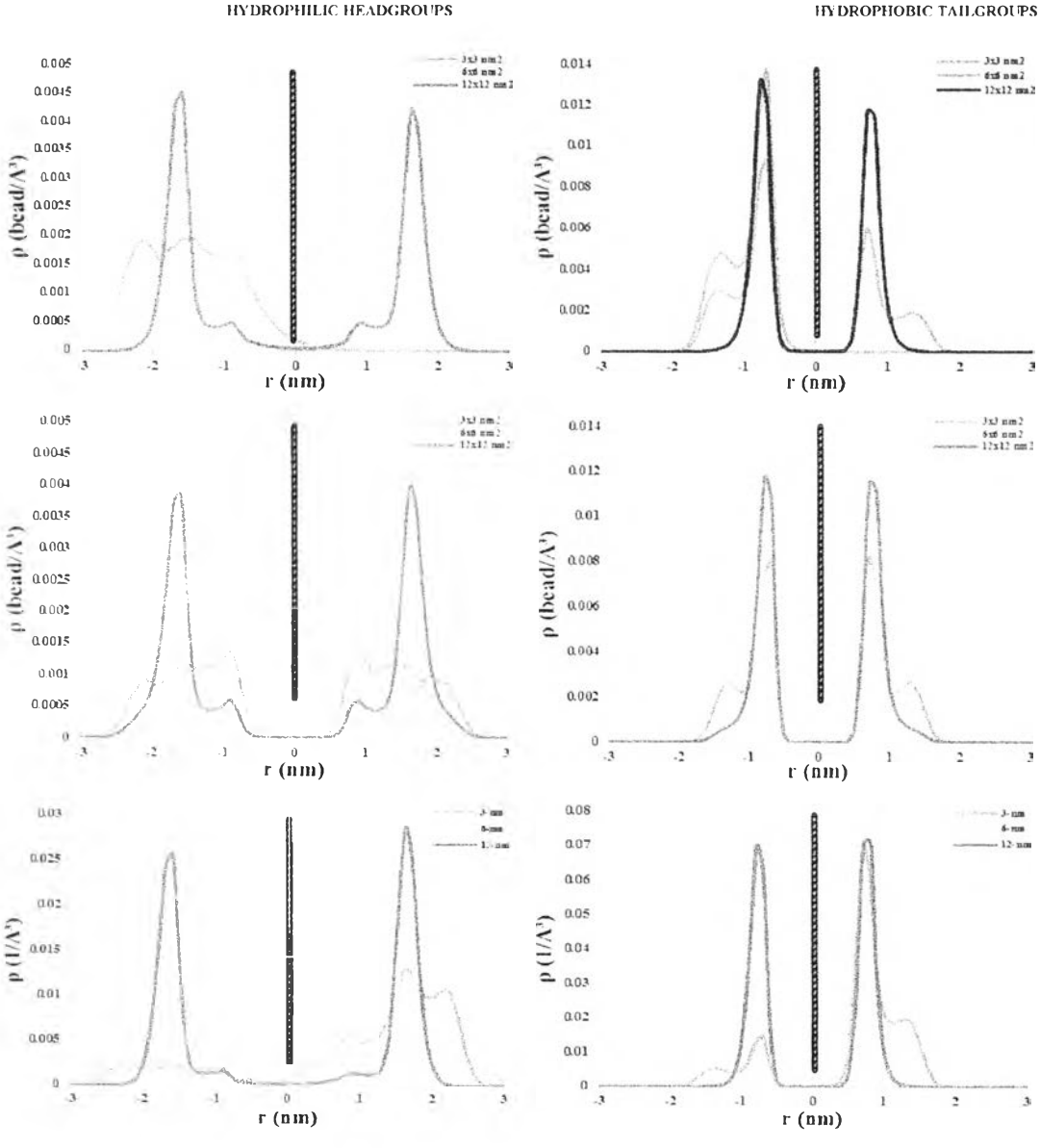

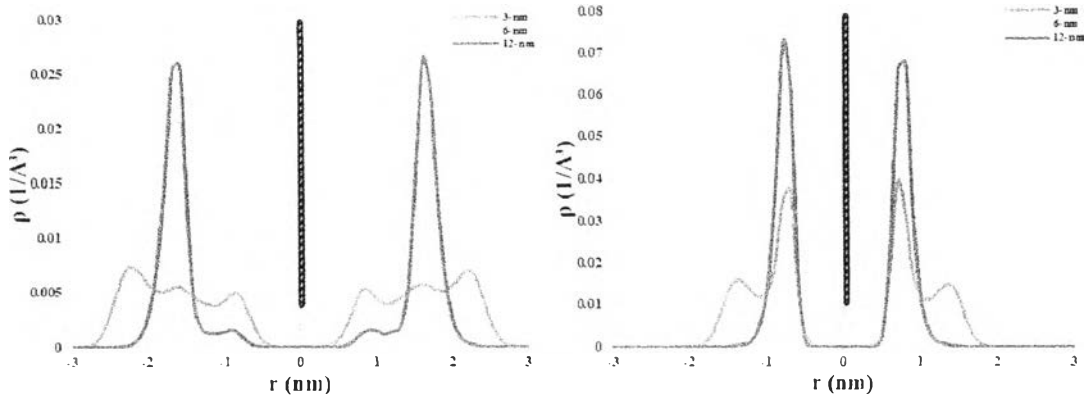

Figure 4.9 Density profiles of SDS headgroups (left panel) and tailgroups (right panel), perpendicular to GS (First row), GOS (Second row), GN (Third row) and GON (Fourth row).

The profiles on the GSs and GOSs are not symmetrical like the profiles on GNs and GONs. This is due to the movement of the aggregate from one side of the sheet, or the nano-ribbon, to another side. Nevertheless, the total coverage of the whole nano-particles remained at 0.5 nm^2/SDS molecule, since no SDS molecules desorbed from the surface. The average numbers of surfactants adsorbed on each side of the nano-particles during the last 0.1275 ns of the simulations are shown in **Table 5**. The top side is the side that faces the positive Z-direction, and the bottom side is the side that faces the negative Z-direction.

Table 4.2 The population analysis for SDS molcules on each side of the nano-particles in the last 0.1275 ns of the simulations

Type	Dimension	Average Number of SDS molecules adsorbed on top side	Average surface coverage on top side (nm^2/SDS molecule)	Average Number of SDS molecules adsorbed on bottom side	Average surface coverage on bottom side (nm^2/SDS molecule)
GS	3×3 nm^2	0	0	36	0.25
	6×6 nm^2	54	0.67	90	0.4
	12×12 nm^2	272	0.53	304	0.47
GOS	3×3 nm^2	18	0.5	18	0.5
	6×6 nm^2	72	0.5	72	0.5
	12×12 nm^2	288	0.5	288	0.5
GN	3-nm wide	268	0.31	65	1.28
	6-nm wide	273	0.61	393	0.42
	12-nm wide	674	0.493	657	0.506
GON	3-nm wide	167	0.498	166	0.5
	6-nm wide	333	0.5	333	0.5
	12-nm wide	666	0.499	665	0.5

In the hydrophobic tailgroup density profiles, the common feature is the first and highest peak at r = 0.7 nm and 0.8 nm. The peak at 0.7 nm is observed on the sheets and nano-ribbons, which have multi-layered aggregates. This peak indicates the parallel layer of the surfactants at the base of the aggregate. Another peak at 0.8 nm is observed on the surfaces that have mono-layered aggregate. The number of peaks in the hydrophobic tailgroup density profiles signifies the number of layers in the aggregate. For example, two peaks in the density profile on the 3x3 nm^2 GOS corresponds to two layers of the aggregate, as seen in Fig. 10. The density profiles of the multi-layered aggregates display the peaks with periodic interval of 0.7 nm. The tailgroup density is lower as it is more away from the sheet (Tummala, Grady et al. 2010) and reaches zero after r = 1.8 nm. It reduces because there are fewer surfactants on top of the aggregate, than at the bottom of the aggregate. The density profile of the mono-layered aggregate is a single very high peak. It indicates the presence of surfactants in one particular layer, which agrees with the inspection of the snapshots.

The hydrophilic headgroups density profiles indicate the perpendicular height of the aggregate from the surface of the sheets and the ribbons. The multi-layered aggregates have the heights between 2.5-2.8 nm. However, these values have to subtract 0.4 nm, which is the cut-off distance around the carbonaceous surfaces. Therefore the actual aggregate height is between 2.1-2.4 nm. This height is consistent with the morphology of the aggregate, because the height of SDS monolayer cannot be higher than, approximately, 1.8 nm, which is the length of an individual SDS molecule. The height of the aggregate is lower when there are fewer surfactants available in the aggregate. As we compare the height of the aggregate, on the same side of 3x3 nm^2 GS and 3x3 nm^2 GOS, the aggregate on the GS is higher than the aggregate on GOS. This happens, because all surfactants move to one particular side of 3x3 nm^2 GS. The density profiles of the monolayer aggregate have a small peak close to the surface and a consecutive big peak away from the surface. The small peak corresponds to the head beads of the parallel surfactants on the edges of the surface. The large peak represents the head beads of the mono-layered aggregate, with the approximate height of 1.6 nm.

Two-dimensional density profiles of head groups, parallel to the 6x6 nm^2 GS, 6x6 nm^2 GOS, 6-nm-wide GN, and 6-nm-wide GON, are shown in Fig. 13, for comparison. We chose to compare the profiles on the bottom side of 6x6 nm^2 GS and 6x6 nm^2 GOS, because the surface coverage on the bottom sides of both sheets are close to each other, compared with the surface coverage on their bottom sides. We also chose to compare the profiles on the bottom sides of 6-nm-wide GN, and 6-nm-wide GON for the same reason.

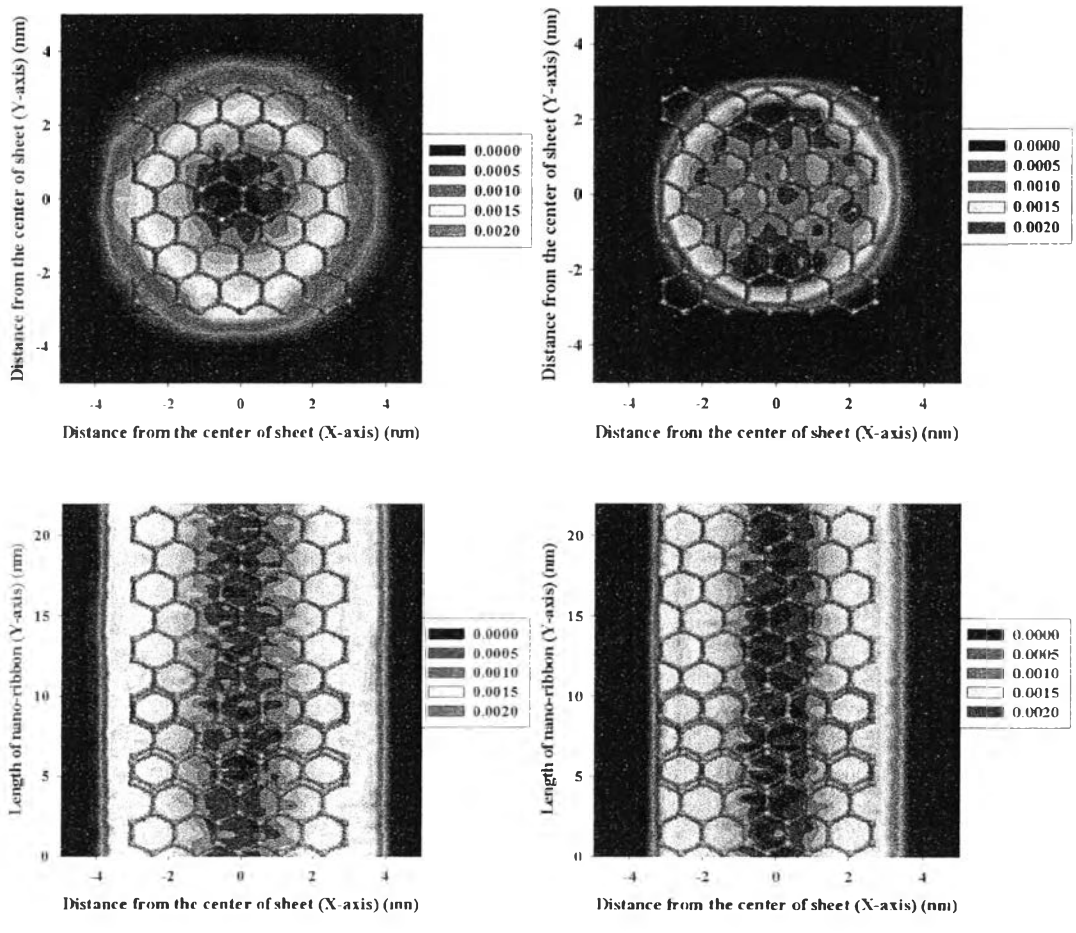

Figure 4.10 Contour plots of SDS headgroups density profiles on top sides of 6×6 nm^2 sheets (Top panel) and on 6-nm-wide nano-ribbons (Bottom panel). The left panel shows the structures without pseudo-oxide edges, and the right panel shows the structures with pseudo-oxide edges.

The density profiles on the oxidized nano-particles (GOS and GON) are smaller than the density profiles on the non-oxidized nano-particles (GS and GN).

The density profile on GOS exhibits large radial high density area in the middle of the sheet. From visual inspection, the surfactants are held on a specific side of the sheet by the pseudo-oxide edges, so they create high density on that particular area over time. On GS, the high density area is also observed in the middle of the sheet, but it is smaller compared with one on GOS. This is due to lack of pseudo-oxide edges that hold surfactants within the boundary. Similarly, the density profile in the middle of the GON shows slightly higher density than the density profile in the middle of the GN. This is due to the same cause. However, the effect is less obvious on GON, because there are only pseudo-oxide edges present along Y-axis only.

4.5 GS Agglomeration

Pairs of GSs of the three different sizes were simulated in SDS-water solution of concentration 99.7 mmol/l for 1.1475 μs. The final configuration of surfactant-covered GSs were duplicated and placed in the new simulation box. The dimension of the box is of 27.72 x 27.72 x 27.72 $Å^3$. The sheets are fixed with initial separation of 12.59 nm, as seen in Fig. 4.11. The simulation box was filled with water. No surfactants molecules is present in the bulk. The initial surface coverage of each duplicated post-adsorption GSs are shown in Table 4.3

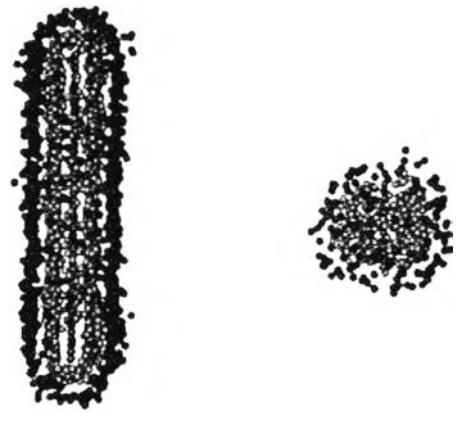

Figure 4.11 Example of initial configuration of the simulation. Water beads are removed for clearer presentation. The blue box represents the periodic boundary condition box.

Table 4.3 Size and initial surface coverage of GSs after surfactant adsorption in the simulated solution

GS size (nm^2)	Initial surface coverage (nm^2/SDS molecule)
3 x 3	0.12
6 x 6	0.22
12 x 12	0.37

The pair of sheets was allowed to diffuse for 1.1475 μs. Each simulation was repeated two times. From each simulation, the agglomeration time, which is the time of which agglomeration occurred, was recorded.

The sheets were considered to agglomerate when they lied parallel close to each other. In this state, only vacuum (Huang et al. 2005), can be observed between them (Shih, Lin et al. 2010). Once they agglomerate, two GSs were together as a single entity (Park and Aluru 2011). The summary of the GSs' size, surface coverage and agglomeration time of each case are shown in Table 4.4.

Table 4.4 Summary of the GSs' sizes, surface coverage and agglomeration time of each simulation. For the cases where agglomeration did not occur, the agglomeration time is notified as N/A

Cases	Surface Coverage (nm^2/SDS molecule)	Agglomeration Time (μs)	Cases	Surface Coverage (nm^2/SDS molecule)	Agglomeration Time (μs)
3×3	0.12 / 0.12	N/A	3×3	0.12 / 0.22	N/A
VS	0.15 / 0.15	N/A	VS	0.15 / 0.27	N/A
3×3	0.2 / 0.2	N/A	6×6	0.2 / 0.37	0.2965013

Table 4.4 Summary of the GSs' sizes, surface coverage and agglomeration time of each simulation. For the cases where agglomeration did not occur, the agglomeration time is notified as N/A (cont.)

Cases	Surface Coverage (nm^2/SDS molecule)	Agglomeration Time (μs)	Cases	Surface Coverage (nm^2/SDS molecule)	Agglomeration Time (μs)
3x3	0.12 / 0.37	N/A	6x6	0.22 / 0.22	N/A
VS	0.15 / 0.46	N/A	VS	0.27 / 0.27	N/A
12x12	0.2 / 0.61	0.408	6x6	0.37 / 0.37	0.1466
6x6	0.22 / 0.37	N/A	12x12	0.37 / 0.37	N/A
VS	0.27 / 0.46	0.77775	VS	0.46 / 0.46	N/A
12x12	0.37 / 0.61	0.14025	12x12	0.61 / 0.61	0.11475

As the amount of surfactants on the GSs reduces, there will be higher probability for the GSs to touch and agglomerate (Islam et al. 2003). There is one interesting case. In the case of 6×6 nm^2 GS versus 6×6 nm^2 GS, the GSs agglomerated when their surface coverage equaled 0.37 nm^2/ SDS molecule. However, in the case of 12×12 nm^2 GS versus 12×12 nm^2 GS, the GSs did not agglomerate when their surface coverage equaled 0.37 nm^2/ SDS molecule. We suspect that this difference is related to the amount of surface available on the nano-particles. At the surface coverage of 0.37 nm^2/SDS molecule, there are 195 surfactants present on 6×6 nm^2 GS, and there are 778 surfactants present on 12×12 nm^2 GS. When there are fewer surfactants, the aggregate is affected by the surrounding water beads. The aggregate rearrange themselves to obtain more curvature (Groot 2000).The rearrangement of results in exposure of the GS to another GS.

However, it is uncertain that the agglomeration of GSs in SDS solution will always give the same results that we have obtained in this simulation. Agglomeration depends on the probability of collision between exposed surfaces of the GSs, which

are related to the many factors, such as displacement of surface aggregate, size of the GSs (Hu, Yu et al. 2013), amount of water present between the GSs (Shih, Lin et al. 2010), distance between the GSs (Park and Aluru 2011).

3.6 Visual inspection of agglomeration mechanism

The step-by-step mechanism of GS agglomeration was studied by Park and Aluru (Park and Aluru 2011). That study showed that the agglomeration is triggered by the slight collision of the GS, followed by sliding of the GS on another GS, stacking with each other. However, their study did not involve any surfactant, and they simulated GSs of one size only

In our simulation, snapshots of the GSs were taken before their agglomeration occurs. From the observation, there are two different approaches to agglomeration in this simulation. The first one is touching of the exposed edges of the GSs, which led the sheets to slide on each other and agglomerate. For simplicity, this mechanism is called "Exposed-Collide-Slide-Agglomerate" mechanism. This mechanism assembles the result from the study by Park and Aluru (Park and Aluru 2011) The step-by-step representation of this mechanism is shown in Fig. 4.13

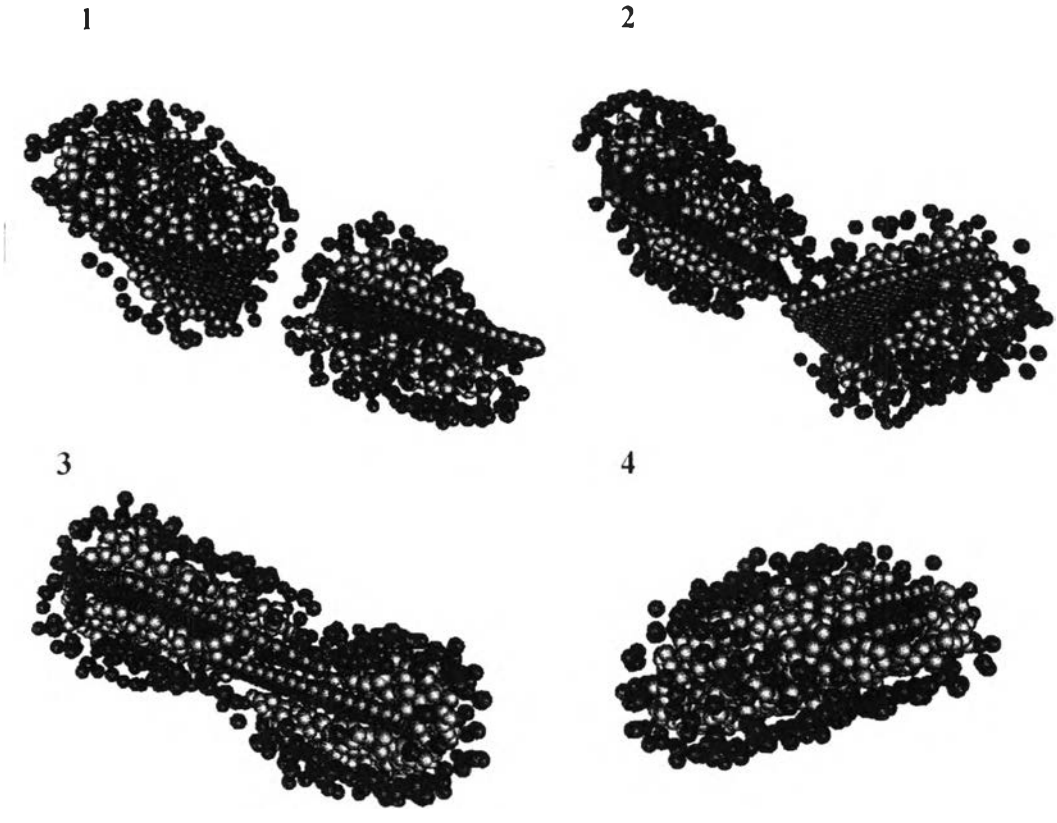

Figure 4.13 Snapshots taken during the agglomeration between 6×6 nm^2 GSs, whose surface coverage were 0.37 nm^2/ SDS molecule (accounting to 60% of the initial surface coverage). The top left diagram shows the "Exposed" phase, when the surfaces of both GSs were partially not covered with SDS aggregate. The top right diagram shows the "Collide" phase, when the bare GSs surfaces touched each other. The bottom left diagram shows the "Slide" phase, when the GSs slided parallel to each other and the bottom right diagram shows the "Agglomerate" phase, when the sheets were covered with SDS agglomerate and become a single bulk.

In addition to the mechanism above, another mechanism is found in our simulation. The second approach is similar to the first approach, but instead of sliding, the sheet flips and adheres with another sheet. The simplified name given to this mechanism is "Exposed-Collide-Flip-Agglomerate". The main difference between "Sliding" and "Flipping" is, during sliding, the GS uses its bare edge to push the agglomerate on another GS, as it slides, but for "Flipping", the GS turns and forces the agglomerate

that still remains between the sheets, inside the turning angle, out. The mechanism is shown in Fig. 4.14

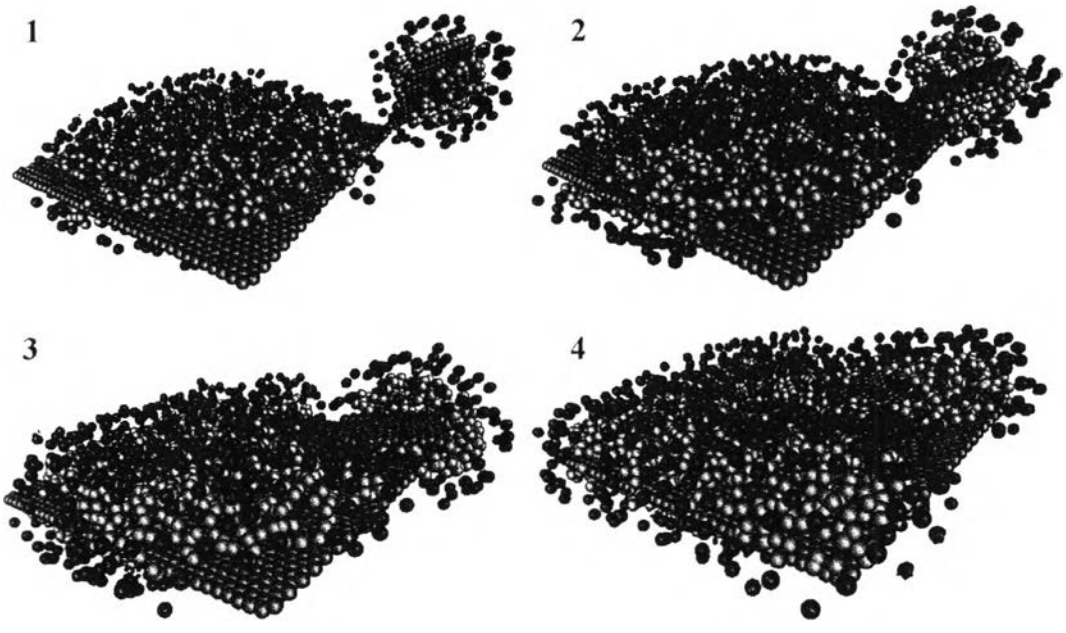

Figure 4.14 Snapshots taken during the agglomeration between 3×3 nm^2 GS and 12×12 nm^2 GS, whose surface coverage were 0.2 nm^2/ SDS molecule and 0.61 nm^2/ SDS molecule (accounting to 60% of their initial surface coverage). The top left diagram shows the "Exposed" phase, when the surfaces of both GSs were not covered with SDS aggregate. The top right diagram shows the "Touch" phase, when the bare GSs surfaces touched each other. The bottom left diagram shows the "Flip" phase, when the 3×3 nm^2 GS turned and the aggregate between the sheets was squeezed out. The bottom right diagram shows the "Agglomerate" phase, when the sheets were covered with SDS agglomerate and become a single entity.

The magnification of the "Sliding" process is shown in the Fig. 4.15

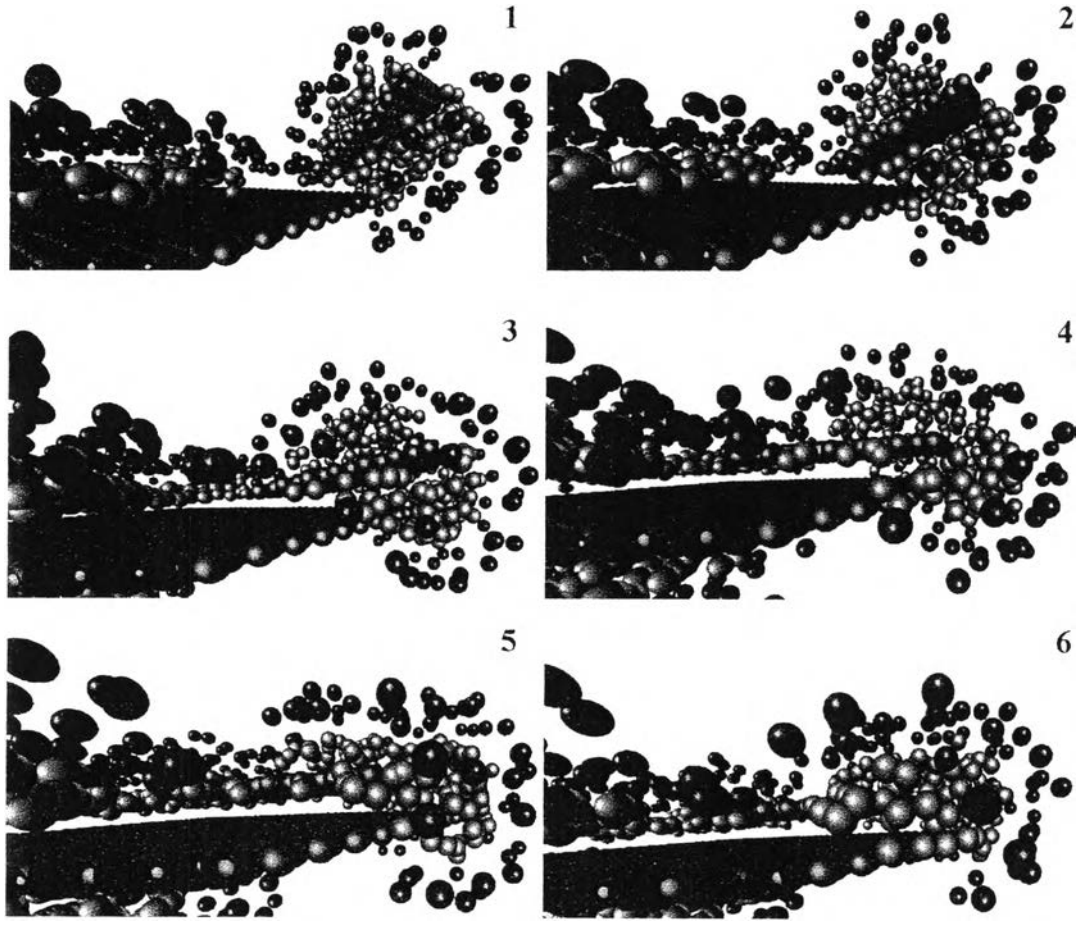

Figure 4.15 Magnification of the snapshots taken during the "Flipping" step in the mechanism.

In order to gain the understanding of what leads to different agglomeration mechanisms, every agglomerated case were categorized as shown in table 4.5

Table 4.5 Categories of agglomerated cases

Case	Surface coverages (nm^2/SDS molecule)	Agglomeration mechanism
3×3 VS 6×6	0.2 / 0.37	Exposed-Collide-Flip-Agglomerate
3×3 VS 12×12	0.2 / 0.61	Exposed-Collide-Flip-Agglomerate
6×6 VS 6×6	0.37 / 0.37	Exposed-Collide-Slide-Agglomerate
6×6 VS 12×12	0.27 / 0.46	Exposed-Collide-Flip-Agglomerate
6×6 VS 12×12	0.37 / 0.61	Exposed-Collide-Flip-Agglomerate
12×12 VS 12×12	0.61 / 0.61	Exposed-Collide-Slide-Agglomerate

The trend of the agglomeration implies that when the sheets have equal size, they are likely to go through exposed-Touch-slide-agglomerate mechanism, and when the size is different, the sheets go through exposed-Touch-flip-agglomerate mechanism. However, it is difficult to generalize our observation, since there are only 6 results.